PERFORMANCE OF PARALLEL CODE ACQUISITION SCHEMES FOR MULTICARRIER CDMA OVER FREQUENCY-SELECTIVE RAYLEIGH FADING CHANNELS

Lie-Liang Yang and Lajos Hanzo

Dept. of ECS, University of Southampton, SO17 1BJ, UK.
Tel: +44-703-593 125, Fax: +44-703-594 508
Email: lh@ecs.soton.ac.uk, http://www-mobile.ecs.soton.ac.uk

ABSTRACT

In this contribution we investigate the issue of pseudo-noise (PN) code acquisition in a multi-carrier CDMA (MC-CDMA) system, which is suitable for high data rate transmissions. Specially, we investigate the acquisition performance of a pure parallel acquisition scheme over frequency-selective fading channels under the multiple in-phase states (H_1 cells) hypothesis, considering both noncoherent equal gain combining (EGC) and selection combining (SC) of the correlator outputs associated with the sub-carriers. It is demonstrated that the acquisition performance of the MC-CDMA scheme is better than that of the equivalent single-carrier CDMA (SC-CDMA) benchmarker, when EGC is employed, and it is similar to that of the single-carrier CDMA scheme, when SC is employed.

1. INTRODUCTION

Recently multi-carrier code-division multiple-access (MC-CDMA) has been proposed for example for the third generation (3G) cdma2000 system [1], which is based on a combination of CDMA and orthogonal frequency division multiplexing (OFDM) based signalling. The advantages of MC-CDMA include high bandwidth efficiency, frequency diversity, reduced-speed parallel signal processing requirements and powerful interference rejection capability at high data rates [2, 3, 4]. The performance of MC-CDMA systems designed for achieving different tasks has been widely studied [2, 3, 4], but the renowned individual contributors are too numerous to name. However, in all of these papers, the investigations were based on the assumption that there was perfect synchronization between the pseudo-noise (PN) spreading code of the received signal and the locally generated despreading code of the receiver. The initial synchronization issues of MC-CDMA have so far only been treated in [5], where frequency diversity was achieved by transmitting the same narrow-band CDMA signal on all subcarriers.

This work has been performed in the framework of the Pan-Euroepan IST project IST-1999-12070 (TRUST), which is partly funded by the European Union. The authors would like to acknowledge the contributions of their colleagues, although the views expressed are those of the authors.

The financial support of the EPSRC, Swindon, UK is also gratefully acknowledged.

PIMRC'2000, 18-22 Sept. 2000, London, UK

0-7803-6465-5/00 $10.00 © 2000 IEEE

In this contribution, we consider the performance of a parallel code acquisition scheme over frequency-selective Rayleigh fading channels, which is applicable to MC-CDMA systema. The contributions of this paper are summarized as follows:

- The performance of pure parallel acquisition schemes is evaluated for a high data rate MC-CDMA system, where the transmitted data bits are serial-to-parallel converted for transmission in a number of parallel streams. In this type of MC-CDMA, frequency-selective fading may be encountered not only in the context of different subcarriers, but also for signals transmitted on the same subcarrier, since the bandwidth of the direct-sequence (DS) spread signal on each subcarrier may be wider, than the channels' coherence bandwidth [3].

- In most previous initial synchronization studies a single correct synchronization cell (H_1 cell) was assumed [5, 6]. However, in practice, there are typically multiple H_1 cells in mobile communication environments, since the search step size is expected to be smaller than one PN code chip duration (typically 1/2 PN code chip). The search step-size of 1/2-chip results in an H_1 cell at both sides of the perfectly aligned position. Therefore, invoking the conventional single H_1 cell approach provides a limited-accuracy performance estimation [7]. Hence, the multiple H_1 cell hypothesis is used in our analysis.

- In numerous CDMA systems the transmitter aids the initial acquisition by transmitting the phase-coded carrier signal without data modulation at the commencement of each transmission. In this MC-CDMA scenario the outputs of the noncoherent subcarrier correlators associated with the same phase of the local PN code replica can be combined, provided that all subcarriers employ the same PN spreading sequence. In our analysis, two noncoherent combining schemes [5] - namely equal gain combining (EGC) and selection combining (SC) - are investigated and compared. Furthermore, the acquisition performance of both EGC and SC is compared to that of the equivalent SC-CDMA schemes over frequency- selective Rayleigh fading channels.

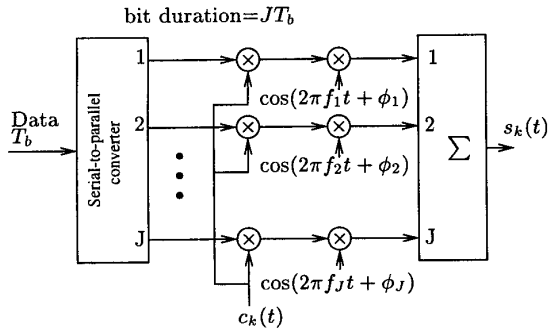

Figure 1: The transmitter diagram of the multi-carrier DS-CDMA systems.

2. SYSTEM MODEL

2.1. The Transmitter and Channel Model

The kth user's transmitter is shown in Fig.1 in the framework of the MC-CDMA system considered, which is similar to that analysed in [3], except that no interleaving across different subcarriers is assumed in our analysis. However, the analysis in this contribution can be readily extended to the PN code acquisition study of MC-CDMA systems using interleaving across the different subcarriers. As shown in Fig.1, the bit stream having a bit duration of T_b is serial-to-parallel converted to J parallel streams at the transmitter. The bit duration of each stream modulated on to the subcarriers hence becomes $T_{bs} = JT_b$. All data streams are spread by the same signature sequence, which is given by $c_k(t) = \sum_{n=-\infty}^{\infty} c_n^{(k)} P_{JT_c}(t - nJT_c)$, where $\left\{c_n^{(k)}\right\}$ is a random sequence with $c_n^{(k)}$ taking values of ± 1 with equal probability. We assume that the system supports K users and that all users have J number of subcarriers. Moreover, we assume that the first user is the user-of-interest, while the other users are synchronized and reached the data transmission stage. Furthermore, we assume that ideal power control is employed for all the communicating users. Consequently, after modulating the corresponding subcarrier, the transmitted signal for user k can be expressed as:

$$s_k(t) = \sum_{j=1}^{J} \sqrt{2P_k} b_k(t) c_k(t) \cos(2\pi f_j t + \phi_{jk}), \qquad (1)$$

where the subcarrier data stream $b_k(t) = \sum_{i=-\infty}^{\infty} b_i^{(k)} P_{JT_b}(t - iJT_b)$ consists of a sequence of mutually independent rectangular pulses of duration $T_{bs} = JT_b$ and of amplitude +1 or -1 having an equal probability. Furthermore, the associated user powers are $P_1 = P_r$, while $P_k = P_I$ for $k \neq 1$, where P_k is the subcarrier's transmitting power of user k. Lastly, f_j is the jth subcarrier frequency and ϕ_{jk} is the random phase of each subcarrier. In the following analysis - for the sake of simplicity – we assume that there exists no spectral overlap between the spectral main-lobes of two adjacent subcarriers [5], and hence there exists no adjacent-channel interference between subcarriers. More explicitly, interference is inflicted only, when an interfering user activates the same subcarrier, as the reference user. Let $N = JT_b/JT_c = T_b/T_c$ be the length of the spreading sequence $\left\{c_n^{(k)}\right\}$, where T_b and T_c are the corresponding bit duration and chip duration of the equivalent SC-CDMA system corresponding to $J = 1$. Consequently, both the equivalent SC-CDMA and the MC-CDMA systems considered have the same information rate, the same system bandwidth as well as the same PN spreading sequence length, which allows their direct comparison by comparing their detection probabilities.

The channel model considered is the frequency selective Rayleigh fading channel having a channel impulse response (CIR) matched to user k and subcarrier j expressed as [8]:

$$h_{kj}(t) = \sum_{l=0}^{L-1} \alpha_{kjl} \delta(t - lJT_c) \exp\left(-i\psi_{kjl}\right), \qquad (2)$$

where the L tap weights $\{\alpha_{kjl}\}$ are assumed to be independent identical distributed (iid) Rayleigh random variables with a probability density function (PDF) given by [8]:

$$f_{\alpha_{kjl}}(x) = \frac{2x}{\Omega} \exp\left(-\frac{x^2}{\Omega}\right), \; x \geq 0, \qquad (3)$$

where $\Omega = E[\alpha_{kjl}^2]$, lJT_c represents the channel-delay, and lastly, the phases $\left\{\psi_{kjl}\right\}$ in Eq.(2) are assumed to be iid random variables uniformly distributed in $[0, 2\pi]$. Then, based on the assumption of experiencing slow envelope fluctuations with respect to the integral dwell-time of the receiver, the received signal can be expressed as:

$$\begin{aligned} r(t) &= \sum_{j=1}^{J} \sum_{l=0}^{L-1} \sqrt{2P_r} \alpha_{1jl} c_1(t - \tau_1 - lJT_c) \\ &\quad \cdot \cos(2\pi f_j t + \theta_{1jl}) \\ &+ \sum_{k=2}^{K} \sum_{j=1}^{J} \sum_{l=0}^{L-1} \sqrt{2P_k} \alpha_{kjl} b_k(t - \tau_k - lJT_c) \\ &\quad \cdot c_k(t - \tau_k - lJT_c) \cos(2\pi f_j t + \theta_{kjl}) \\ &+ n(t), \end{aligned} \qquad (4)$$

where τ_k is the relative time delay between the user's transmitted signals associated with an asynchronous transmission scheme, $\theta_{kjl} = \phi_{jk} - \psi_{kjl} - 2\pi f_j(\tau_k + lJT_c)$ is a phase term, which is modeled with the aid of iid random variables uniformly distributed in the interval $[0, 2\pi]$ for different values of j, k and l, while $n(t)$ represents the Additive White Gaussian Noise (AWGN) with a double-sided power spectral density of $N_0/2$.

2.1.1. Parallel Code-Acquisition

We consider a pure parallel implementation of the maximum-likelihood (ML) acquisition scheme, as in [6], where all possible PN code phases of the received signal are tested simultaneously. We assume that the acquisition search step size for the MC-CDMA system concerned is $JT_c/2$, and that there are L resolvable paths. Hence, for a PN sequence having an uncertainty region of q cells in the AWGN channel, the total number of cells to be searched in the L-tap dispersive fading channel is $(q \cdot \frac{JT_c}{2} + (L-1)JT_c)/\frac{JT_c}{2} = q + 2(L-1)$ and the number of H_1 cells is $LJT_c/JT_c/2 = 2L$, where $(L-1)JT_c$ represents the maximum delay-spread of the L-tap fading channel. Let $\{Z_0, Z_1, \ldots, Z_{q+2L-3}\}$ denote the

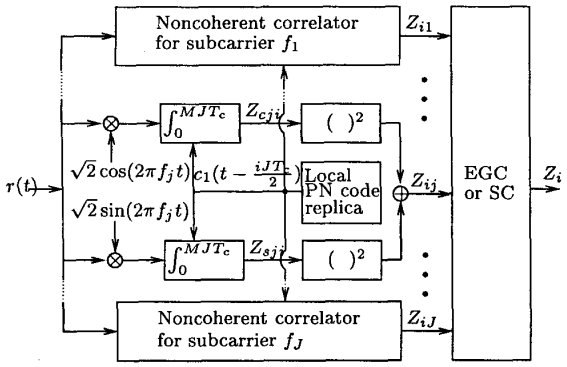

Figure 2: Schematic of generating the decision variable Z_i for the multi-carrier DS-CDMA code-acquisition system.

decision variables corresponding to all the $q+2(L-1)$ number of cells in the uncertainty region of the PN code to be acquired. The block diagram of the proposed scheme used to generate the decision variable Z_i is shown in Fig.2. The philosophy of the parallel search scheme considered is that, the largest decision variable of $\{Z_0, Z_1, \ldots, Z_{q+2L-3}\}$ is selected, which is then forwarded to the associated phase verification mode. If this code phase is confirmed during the verification mode, acquisition is declared. Otherwise, if the largest decision variable of the set $\{Z_0, Z_1, \ldots, Z_{q+2L-3}\}$ cannot be confirmed by the verification mode, then a set of $q+2(L-1)$ new decision variables is collected, and the above process is repeated.

In the MC-CDMA system of Fig.1 all subcarriers employ the same PN spreading sequence. Furthermore, no data modulation is imposed during the acquisition stage. Then, the outputs of those from the set of the J noncoherent subcarrier correlators seen in Fig.2, which are associated with the same specific phase of the local PN code replica can be combined. In this contribution, two noncoherent combining schemes - namely EGC and SC - will be investigated. Since the PN code chip rate of the MC-CDMA system using J subcarriers is a factor of J lower, than that of the corresponding single-carrier system, the number of chip contributions collected during the integration period is also reduced by a factor of J. Let $\tau_D = MJT_c$ be the integration dwell-time for both the MC-CDMA and the SC-CDMA systems considered. Then, it can be shown that for the MC-CDMA system the average energy captured by the correlator of Fig.2 during the integration dwell-time is reduced to $1/J$ times that for the corresponding SC-CDMA system. However, since the chip rate of the SC-CDMA system is J times that of the MC-CDMA system, the number of resolvable paths will be at least JL, where L represents the number of resolvable paths of the corresponding MC-CDMA system. Moreover, since the acquisition search step size is $T_c/2$, which is a factor of J lower, than the search step size $JT_c/2$ of the MC-CDMA system, in a SC-CDMA system the number of cells to be searched in the uncertainty region is $q+2(JL-1)$ and the number of H_1 cells is $2JL$. Bearing in mind these relations between the multi-carrier and single-carrier DS-CDMA systems, let us now derive the detection probability for both the EGC and SC schemes. We proceed by deriving the statistics of the decision variables.

3. DECISION VARIABLE STATISTICS

Since we have assumed that there exists no spectral overlap between two adjacent subcarriers, hence the statistics associated with subcarrier f_j are identical to those of a SC-CDMA system over the multipath fading channel [7]. The output variable of Fig.2 matched to the subcarrier f_j can be expressed as:

$$\begin{aligned} Z_{ij} &= Z_{cji}^2 + Z_{sji}^2 \\ &= \left[\int_0^{MJT_c} r(t)c_1(t-iJT_c/2)\sqrt{2}\cos(2\pi f_j t)dt\right]^2 \\ &+ \left[\int_0^{MJT_c} r(t)c_1(t-iJT_c/2)\sqrt{2}\sin(2\pi f_j t)dt\right]^2, \end{aligned} \quad (5)$$

where $i = 1, 2, 3, \ldots, q+2(L-1)$, $j = 1, 2, \ldots, J$. It can be shown that both Z_{cji} and Z_{sji} can be approximated by Gaussian random variables having normalized means given by [7] $\frac{3}{4}\alpha_{1jl}\cos\theta_{ijl}$ and $\frac{3}{4}\alpha_{1jl}(-\sin\theta_{ijl})$, if an H_1 hypothesis is being tested, and zero, if an H_0 hypothesis being tested. The normalized variance for both Z_{cji} and Z_{sji} is given by [7] $\sigma_o^2 = \frac{(L-1)\Omega}{3M} + \frac{(K-1)L\rho\Omega}{3M} + \frac{1}{2M\gamma_c}$, where $\gamma_c = E_c/N_0$ and E_c is the chip energy. Hence, assuming that Z_{ij} in Fig.2 constitutes an H_1 sample, the PDF of Z_{ij} conditioned on a given α_{1jl} is described by the chi-square distribution with two degrees of freedom. After removing the conditioning on a specific fading attenuation α_{1jl} with the aid of Eq.(3), this PDF can be expressed as:

$$f_{Z_{ij}}(y|H_1) = \frac{1}{2+\overline{\gamma}_c^2}\exp\left(-\frac{y}{2+\overline{\gamma}_c^2}\right), \quad (6)$$

where $\overline{\gamma}_c$ is the average signal-to-noise ratio per chip (SNR/chip) given by [7]

$$\overline{\gamma}_c = \frac{3}{4}\left[\frac{(L-1)}{3M} + \frac{(K-1)L\rho}{3M} + \frac{1}{2M\Omega\gamma_c}\right]^{-1/2}, \quad (7)$$

and $\rho = P_I/P_T$.

By contrast, when Z_{ij} constitutes an H_0 sample, Z_{ij} in Fig.2 obeys the central chi-square distribution and its normalized PDF can be expressed as [8]:

$$f_{Z_{ij}}(y|H_0) = \frac{1}{2}\exp\left(-\frac{y}{2}\right). \quad (8)$$

Consequently, for an EGC scheme the decision variable Z_i is given by the sum of the synchronization outputs $\{Z_{ij}\}$ for $j = 1, 2, \ldots, J$ seen in Fig.2, ie $Z_i = \sum_{j=1}^{J} Z_{ij}$. Again, Eq.(6) and Eq.(8) are described by the central chi-square distribution with two-degrees of freedom and variance of $(2+\overline{\gamma}_c^2)/2$ or unity for the H_1 or H_0 cell hypothesis, respectively. Hence, Z_i of Fig.2 obeys the central chi-square distribution with $2L$ degrees of freedom. Assuming that the H_1 hypothesis is being tested, the PDF of Z_i can be expressed as [8]:

$$f_{Z_i}(y|H_1) = \frac{1}{(2+\overline{\gamma}_c^2)^J(J-1)!}y^{J-1}\exp\left(-\frac{y}{2+\overline{\gamma}_c^2}\right). \quad (9)$$

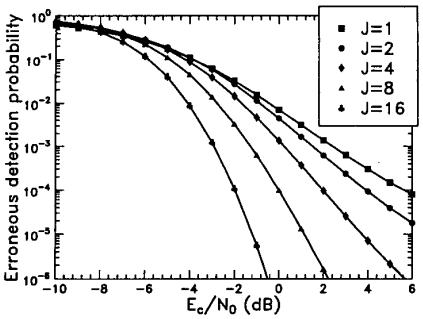

Figure 3: **EGC**: Erroneous detection probability versus SNR/chip performance for the parallel acquisition scheme over the frequency-selective Rayleigh fading channel of Eq.(2) using the parameters $N = 128, q = 256, K = 1, \rho = 1.0, L_p = 16, M_p = 128, L = L_p/J, M = M_p/J$ computed from Eq.(17) with P_D given by Eq.(14).

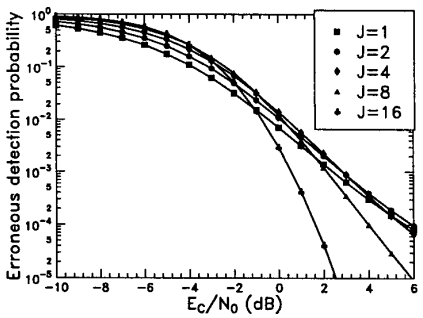

Figure 4: **SC**: Erroneous detection probability versus SNR/chip performance for the parallel acquisition scheme over the frequency-selective fading channel of Eq.(2) using the parameters $N = 128, q = 256, K = 1, \rho = 1.0, L_p = 16, M_p = 128, L = L_p/J, M = M_p/J$ computed from Eq.(17) with P_D given by Eq.(16).

By contrast, upon assuming that a H_0 hypothesis is being tested, the PDF of Z_i can be formulated as [8]:

$$f_{Z_i}(y|H_0) = \frac{1}{2^J(J-1)!} y^{J-1} \exp\left(-\frac{y}{2}\right). \quad (10)$$

Having considered EGC, the output of the SC scheme is given by the highest one of its inputs, which is expressed as $Z_i = \max\{Z_{i1}, Z_{i2}, \ldots, Z_{iJ}\}$. It can be shown that the SC-assisted PDFs conditioned on testing the H_1 and H_0 cells can be expressed, respectively, as:

$$f_{Z_i}(y|H_1) = \frac{J}{2+\overline{\gamma}_c^2} \exp\left(-\frac{y}{2+\overline{\gamma}_c^2}\right) \cdot \left[1 - \exp\left(-\frac{y}{2+\overline{\gamma}_c^2}\right)\right]^{J-1}, \quad (11)$$

$$f_{Z_i}(y|H_0) = \frac{J}{2} \exp\left(-\frac{y}{2}\right) \left[1 - \exp\left(-\frac{y}{2}\right)\right]^{J-1}. \quad (12)$$

4. DETECTION PROBABILITY

The detection probability is defined as the probability that the largest of the decision variables $\{Z_0, Z_1, \ldots, Z_{q+2L-3}\}$ - which are associated with the $q + 2(L-1)$ number of cells in the uncertainty region - corresponds to one of the $2L$ number of H_1 cells. Hence, the detection probability can be expressed as:

$$P_D = 2L \int_0^\infty f_{Z_i}(y|H_1) \left[\int_0^y f_{Z_j}(x|H_1)dx\right]^{2L-1} \cdot \left[\int_0^y f_{Z_k}(x|H_0)dx\right]^{q-2} dy. \quad (13)$$

Consequently, substituting $f_{Z_i}(x|H_1)$ from Eq.(9) and $f_{Z_k}(x|H_0)$ from Eq.(10) into Eq.(13), the detection probability using EGC can be expressed as:

$$P_D = 2L \int_0^\infty \frac{1}{(2+\overline{\gamma}_c^2)^J (J-1)!} y^{J-1} \exp\left(-\frac{y}{2+\overline{\gamma}_c^2}\right) \times \left[1 - \exp\left(-\frac{y}{2+\overline{\gamma}_c^2}\right) \sum_{k=0}^{J-1} \frac{1}{k!} \left(\frac{y}{2+\overline{\gamma}_c^2}\right)^k\right]^{2L-1} \times \left[1 - \exp\left(-\frac{y}{2}\right) \sum_{k=0}^{J-1} \frac{1}{k!} \left(\frac{y}{2}\right)^k\right]^{q-2} dy. \quad (14)$$

Similarly, upon substituting $f_{Z_i}(x|H_1)$ from Eq.(11) and $f_{Z_k}(x|H_0)$ from Eq.(12) into Eq.(13), we obtain the detection probability using SC, which can be expressed as:

$$P_D = \frac{2LJ}{2+\overline{\gamma}_c^2} \int_0^\infty \exp\left(-\frac{y}{2+\overline{\gamma}_c^2}\right) \cdot \left[1 - \exp\left(-\frac{y}{2+\overline{\gamma}_c^2}\right)\right]^{2LJ-1} \cdot \left[1 - \exp\left(-\frac{y}{2}\right)\right]^{(q-2)J} dy. \quad (15)$$

Upon expanding Eq.(15), finally, the detection probability using SC can be expressed as:

$$P_D = 2LJ \sum_{i=0}^{2LJ-1} \sum_{j=0}^{(q-2)J} \binom{2LJ-1}{i} \binom{(q-2)J}{J} \cdot \frac{(-1)^{i+j}}{1+(i+j)+j\overline{\gamma}_c^2/2}. \quad (16)$$

The erroneous detection probability of EGC or SC is given by:

$$P_e = 1 - P_D, \quad (17)$$

where P_D is the detection probability given by Eq.(14) or by Eq.(16) for EGC or SC, respectively. Note that the erroneous detection probability is essentially synonymous to the false-alarm probability for the parallel acquisition system considered, since Eq.(17) implies that the largest decision variable Z_i from the set of $\{Z_0, Z_1, \ldots, Z_{q+2L-3}\}$ corresponds to an H_0 cell.

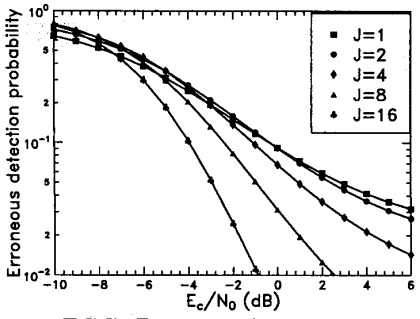

Figure 5: **EGC**: Erroneous detection probability versus SNR/chip performance for the parallel acquisition scheme over the frequency-selective Rayleigh fading channel of Eq.(2) using the parameters $N = 128, q = 256, K = 3, \rho = 1.0, L_p = 16, M_p = 128, L = L_p/J, M = M_p/J$ computed from Eq.(17) with P_D given by Eq.(14).

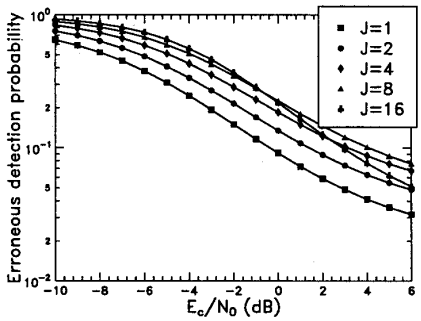

Figure 6: **SC**: Erroneous detection probability versus SNR/chip performance for the parallel acquisition scheme over the frequency-selective Rayleigh fading channel of Eq.(2) using the parameters $N = 128, q = 256, K = 3, \rho = 1.0, L_p = 16, M_p = 128, L = L_p/J, M = M_p/J$ computed from Eq.(17) with P_D given by Eq.(16).

5. NUMERICAL RESULTS

The probability of erroneous code phase detection for EGC and SC over the frequency-selective fading channel of Eq.(17) is shown in Fig.3 and Fig.4, respectively. In Fig.3 and Fig.4, L_p and M_p represent the number of resolvable paths and the number of chips during the integral dwell-time for SC-CDMA ($J = 1$), respectively. Moreover, since the number of resolvable paths for the MC-CDMA scheme studied equals to $L = L_p/J$, we have $L = 1$ for $J = L_p$. In this case, the MC-CDMA system considered is equivalent to the system discussed in [5]. From the results we observe that over the multipath fading channels considered, the initial synchronization performance of the MC-CDMA system using EGC is better, than that of the SC-CDMA system. Furthermore, the MC-CDMA system using selection combining and the single-carrier CDMA system exhibit a similar performance over the multipath fading channel of Eq.(2) in the SNR/chip range considered. Interestingly, the single-carrier CDMA system outperforms the MC-CDMA system, if the SNR/chip is low, while this situation is reversed, when the SNR/chip is high. This issue can be readily explained upon invoking Eq.(15) combined with Eq.(7). If we let $L_p = JL$ in Eq.(15), then we have:

$$P_D = \frac{2L_p}{2+\overline{\gamma}_c^2} \int_{h'}^{\infty} \exp\left(-\frac{y}{2+\overline{\gamma}_c^2}\right) \cdot \left[1 - \exp\left(-\frac{y}{2+\overline{\gamma}_c^2}\right)\right]^{2L_p-1} \cdot \left[1 - \exp\left(-\frac{y}{2}\right)\right]^{(q-2)J} dy. \quad (18)$$

It can be shown that P_D in Eq.(18) will decrease, as the number of subcarriers, J, increases. However, the average received SNR/chip, $\overline{\gamma}_c$, increases when J increases, since the number of resolvable paths $L = L_p/J$ of each subcarrier decreases, when J increases. Consequently, the two-fold influence of J results in the observation stated in the context of Fig.4.

In contrast to Fig.3 and Fig.4, where the number of active users was $K = 1$, i.e., no multiuser interference was inflicted, in Fig.5 and Fig.6 we let $K = 3$, i.e., there were two interfering users. The other parameters were the same, as in Fig.3 and Fig.4, which were listed in the captions of the figures. From the results we observe that for the EGC scheme the performance is similar to that of $K = 1$, provided that the SNR/chip is sufficiently high. However, for the SC scheme the single-carrier CDMA system outperforms the MC-CDMA system over the entire SNR/chip range considered.

6. REFERENCES

[1] R. Steele, L. Hanzo (Ed): Mobile Radio Communications: Second and Third Generation Cellular and WATM Systems, John Wiley-IEEE Press, 2nd edition, 1999, ISBN 07 273-1406-8

[2] R. Prasad and S. Hara, "Overview of multicarrier CDMA," *IEEE Communications Magazine*, pp. 126–133, December 1997.

[3] E. A. Sourour and M. Nakagawa, "Performance of orthogonal multicarrier CDMA in a multipath fading channel," *IEEE Transactions on Communications*, vol. 44, pp. 356–367, March 1996.

[4] L.-L. Yang and L. Hanzo, "Blind soft-detection assisted frequency-hopping multicarrier DS-CDMA systems," in *Proc. of IEEE GLOBECOM'99*, (Rio de Janeiro, Brazil), pp. 842–846, December:5-9 1999.[1]

[5] D. Lee and L. B. Milstein, "Analysis of a multicarrier DS-CDMA code-acquisition system," *IEEE Transactions on Communications*, vol. 47, pp. 1233–1244, August 1999.

[6] R. R. Rick and L. B. Milstein, "Parallel acquisition in mobile DS-CDMA systems," *IEEE Transactions on Communications*, vol. 45, pp. 1466–1476, November 1997.

[7] L.-L. Yang and L. Hanzo, "Serial acquisition techniques for DS-CDMA signals in frequency-selective multi-user mobile channels," in *Proc. of IEEE VTC'99*, (Houston, USA), pp. 2398–2402, May 1999.[1]

[8] J. G. Proakis, *Digital Communications*. McGraw Hill, 3rd ed., 1995.

[1] [4, 7]: Also see http://www-mobile.ecs.soton.ac.uk/lly.